

MOL #91462

**Characterization of the Zebrafish *Ugt* Repertoire Reveals a New Class of Drug-metabolizing UDP
Glucuronosyltransferases**

Yuanming Wang, Haiyan Huang, and Qiang Wu

Key Laboratory of Systems Biomedicine (Ministry of Education), Center for Comparative Biomedicine,
Institute of Systems Biomedicine, Shanghai Jiao Tong University, Shanghai 200240, China; (YW, HH,
QW)

State Key Laboratory of Oncogenes and Related Genes, Shanghai Cancer Institute, Renji Hospital, School
of Medicine, Shanghai Jiao Tong University, Shanghai 200240, China; (YW, HH, QW)

Key Laboratory for the Genetics of Developmental and Neuropsychiatric Disorders, Ministry of Education,
Bio-X Center, School of Life Sciences and Technology, Shanghai Jiao Tong University, Shanghai 200240 ,
China (YW, HH, QW)

MOL #91462

Running title: Glucuronidation Activity of the Zebrafish UGT Superfamily

Corresponding Author: Qiang Wu, Shanghai Jiao Tong University, 800 Dongchuan Rd, Minhang,

Shanghai 200240, China; Tel: 86-21-34204300; Fax: 86-21-34204300; E-mail: qwul23@gmail.com

Number of text pages: 43

Number of tables: 3

Number of figures: 5

Number of references: 44

Number of words in *Abstract*: 250

Number of words in *Introduction*: 711

Number of words in *Discussion*: 1223

Abbreviation: 1-naphthol-G, 1-naphthol β -D-glucuronide; 4-MU, 4-methylumbelliferone; 4-MU-G, 4-methylumbelliferyl β -D-glucuronide; 4-NP, 4-nitrophenol; 4-NP-G, 4-nitrophenyl β -D-glucuronide; bilirubin-DG, bilirubin di-acyl- β -D-glucuronide; bilirubin-MG, bilirubin mono-acyl- β -D-glucuronide; BPA, bisphenol A; BPA-G, bisphenol A β -D-glucuronide; diclofenac-G, diclofenac acyl- β -D-glucuronide; DMEM, Dulbecco's modified Eagle medium; DMSO, dimethyl sulfoxide; E₂, β -estradiol; E₂-17G, β -estradiol 17- β -D-glucuronide; E₂-3G, β -estradiol 3- β -D-glucuronide; Endo H, endoglycosidase H; ER, endoplasmic reticulum; HPLC, high-performance liquid chromatography; MPA, mycophenolic acid; MPA-G, mycophenolic acid β -D-glucuronide; PCDH, protocadherin; RT-PCR, reverse transcriptase polymerase chain reaction; testosterone-G, testosterone 17- β -D-glucuronide; TFA, trifluoroacetic acid; t-OP, 4-tert-octylphenol; t-OP-G, 4-tert-octylphenol β -D-glucuronide; UDPGA, UDP glucuronic acid; UGT, UDP glucuronosyltransferase.

MOL #91462

Abstract

The zebrafish genome contains a gene superfamily of 40 *Ugt* genes that can be divided into *Ugt1*, *Ugt2*, and *Ugt5* families. Because the encoded zebrafish UGT proteins do not display orthologous relationships to any of the mammalian and avian UGT enzymes based on molecular phylogeny, it is difficult to predict their substrate specificity. Here, we mapped their tissue-specific expression patterns. We showed that the zebrafish UGT enzymes can be glycosylated. We determined their substrate specificity and catalytic activity toward diverse aglycone substrates. Specifically, we measured mRNA levels of each of the 40 zebrafish *Ugt* genes in 11 adult tissues and found that they are expressed in a tissue-specific manner. Moreover, functional analyses with the donor of UDPGA for each of the 40 zebrafish UGT proteins revealed their substrate specificity toward ten important aglycones. In particular, UGT1A1, UGT1A7, and UGT1B1 displayed good glucuronidation activities toward most phenolic aglycones (4-methylumbelliferone, 4-nitrophenol, 1-naphthol, bisphenol A, and mycophenolic acid) and the two carboxylic acids (bilirubin and diclofenac). Importantly, some members of the UGT5, a novel UGT family identified recently, are capable of glucuronidating multiple aglycones with the donor cofactor of UDPGA. In particular, UGT5A5, UGT5B2, and UGT5E1 glucuronidate phenols and steroids with high specificity toward steroid hormones of estradiol and testosterone, and estrogenic alkylphenols 4-tert-octylphenol. These results shed new insights into the mechanisms by which fish species defend themselves against vast numbers of xenobiotics via glucuronidation conjugations, and may facilitate the establishment of zebrafish as a model vertebrate in toxicological, developmental, and pathological studies.

MOL #91462

Introduction

With a high-quality reference genome assembled and a repertoire of molecular genetics tools available, the zebrafish has become a powerful vertebrate model for human biology and diseases (Howe et al., 2013; Stegeman et al., 2010). The zebrafish has also emerged as a popular toxicological model for drug discovery, endocrinology, and environmental chemical defense studies (James, 2011; Peterson and Macrae, 2012; Stegeman et al., 2010; Tokarz et al., 2013). The UDP-glucuronosyltransferases (UGTs) are an important class of diverse Phase II drug-metabolizing and detoxification enzymes that affect the drug toxicity as well as its oral bioavailability (Meech et al., 2012; Wu et al., 2011). In mammals, UGTs are encoded by two gene clusters: *Ugt1* and *Ugt2* (Mackenzie et al., 2005; Owens et al., 2005). The mammalian *Ugt1* clusters are organized in a tandem array of multiple highly-similar variable exons followed by a single set of four constant exons (Emi et al., 1995; Li and Wu, 2007; Mackenzie et al., 2005; Owens et al., 2005; Ritter et al., 1991; Zhang et al., 2004), similar to the organization of the protocadherin (*Pcdh*) clusters (Wu, 2005). Each *Ugt1* variable exon encodes a signal peptide and the amino-terminal aglycone-recognition domain. The constant exons encode a highly conserved donor-binding domain and the carboxyl-terminal endoplasmic-reticulum (ER)-anchoring transmembrane segment. Alternative splicing from each of the multiple variable first exons to the common set of downstream constant exons generates the enormous molecular diversity required for metabolizing diverse small lipophilic chemicals. In addition, characterization of the genetic variability of the *UGT1* gene cluster in different human populations has revealed ethnic specific diversity of *UGT1* haplotypes and linkage blocks (Maitland et al., 2006; Ménard et al., 2009; Saeki et al., 2006; Thomas et al., 2006; Yang et al., 2012). The mammalian *Ugt2* clusters include three *Ugt2a* genes and about a dozen *Ugt2b* genes (Mackenzie et al., 2005; Owens et

MOL #91462

al., 2005). The mammalian UGT enzymes catalyze the glucuronidation of a vast number of lipophilic endobiotics and xenobiotics with the UDP-glucuronic acid (UDPGA) as a donor cofactor (Meech et al., 2012).

Glucuronidation has long been proven to be an important detoxification pathway for organic pollutants in fish species (Dutton, 1980; Stegeman et al., 2010). Glucuronidation by Phase II enzymes converts endogenous lipophilic metabolites into hydrophilic compounds, which are easily excreted in urine (James, 2011). For example, fish glucuronidate one or both propionic groups of the pigmental bilirubin and excrete the conjugated bilirubin through bile (Clarke et al., 1992; Dutton, 1980). To date, limited information is available on the specific piscine UGT isoforms that are responsible for the glucuronidation of various xenobiotics and endobiotics (Meech et al., 2012; Wu et al., 2011). We recently reported identification of the complete repertoire of 40 *Ugt* genes and 5 *Ugt* pseudogenes in the zebrafish and found that teleosts have many more *Ugt* genes than mammals (Huang and Wu, 2010). Specifically, zebrafish *Ugt* genes can be divided into *Ugt1*, *Ugt2*, and *Ugt5* families. Both *Ugt1* and *Ugt2* clusters are duplicated and organized into variable and constant regions. Every *Ugt1* and *Ugt2* variable exon is separately spliced to a common set of downstream constant exons in respective clusters (Huang and Wu, 2010). In addition, there are a set of 18 zebrafish *Ugt5* genes whose entire open reading frames are encoded by single large exons. These *Ugt5* genes are found in the genomes of teleosts and amphibians but not in mammals and may arise from retrotransposition (Huang and Wu, 2010). The expression patterns and functions of none of these zebrafish *Ugt* genes are known.

MOL #91462

Here we report the expression patterns and catalytical functions of the entire zebrafish *Ugt* repertoire. In particular, we characterized the glucuronidation functions of each of the 40 recombinant zebrafish UGT proteins toward ten important aglycone substrates, including endogenous hormones or metabolites (estradiol, testosterone, and bilirubin), exogenous drugs (4-methylumbelliferone, mycophenolic acid, and diclofenac), as well as environmental toxins (4-nitrophenol, 1-naphthol, 4-tert-octylphenol, and bisphenol A). We demonstrated for the first time that members of the UGT5 family proteins are true glucuronosyltransferase enzymes utilizing UDPGA as the donor substrate. These results have important implications on the catalytic mechanisms by which zebrafish phase II drug-metabolizing UGT enzymes metabolize endobiotics and xenobiotics. Our findings should also facilitate the development of the zebrafish as a model organism for drug screening and environment monitoring.

MOL #91462

Materials and Methods

Materials.

4-Methylumbelliferone (4-MU), diclofenac sodium salt, 4-methylumbelliferyl β -D-glucuronide hydrate (4-MU-G), 4-nitrophenyl β -D-glucuronide (4-NP-G), β -estradiol 3-(β -D-glucuronide) sodium salt (E₂-3G), β -estradiol 17-(β -D-glucuronide) sodium salt (E₂-17G), uridine 5'-diphosphoglucuronic acid triammonium salt (UDPGA), and dimethyl sulfoxide (DMSO) were purchased from Sigma-Aldrich (St. Louis, USA). 1-Naphthol β -D-glucuronide (1-naphthol-G) was purchased from Santa Cruz Biotech (Santa Cruz, USA). β -Estradiol (E₂), testosterone, and bilirubin were purchased from Adamas-beta (Shanghai, China). 4-tert-Octylphenol (t-OP) was purchased from Tokyo Chemical Industry (Tokyo, Japan). Mycophenolic acid (MPA), 4-nitrophenol (4-NP), 1-naphthol, and bisphenol A (BPA) were purchased from Sangon (Shanghai, China). TRIzol reagent and Lipofectamine 2000 were purchased from Invitrogen (Carlsbad, USA). Taq DNA polymerase and ribonuclease-free DNase I were purchased from Takara (Otsu, Japan). AMV reverse transcriptase and pGEM-T Easy vector were purchased from Promega (Fitchburg, USA). Restriction endonucleases, T4 DNA ligase, and endoglycosidase H (Endo H) were purchased from the New England Biolabs (Ipswich, USA). Cell culture medium, fetal bovine serum, and trypsin were purchased from Thermo Fisher Scientific (Waltham, USA). The high-performance liquid chromatography (HPLC)-grade methanol and acetonitrile were purchased from Merck (Darmstadt, Germany).

Methods.

Expression Profiling. We designed an isoform-specific primer pair for each member of the zebrafish *Ugt* repertoire (Supplemental Table S1). The PCR product for each zebrafish *Ugt* gene spans at least one

MOL #91462

intervening intron to avoid contamination from the genomic DNA. The specificity of all of the primer pairs was confirmed by sequencing the amplified PCR product for each member of the zebrafish *Ugt* superfamily. Adult zebrafish (*Danio rerio*) of about 6 months were purchased from the Institute of Biochemistry and Cell Biology, Shanghai Institute of Biological Sciences, Chinese Academy of Sciences. Total RNA was isolated from various tissues of the adult zebrafish with the TRIzol reagent according to the manufacturer's instructions. The zebrafish *Ugt* cDNAs were amplified from total RNA by reverse transcriptase polymerase chain reaction (RT-PCR). 20 μ l of total RNA was treated with ribonuclease-free DNase I at 37°C for 30 min. The first-strand cDNA was synthesized using 1 μ g of DNase I-treated RNA and 0.5 μ g of random primers in the presence of the AMV reverse transcriptase in a final volume of 20 μ l. 1 μ l of the RT product was added to a mixture containing 1 \times PCR buffer, 250 μ M dNTP, 0.25 μ M isoform-specific primers, and 1 unit of Taq DNA polymerase in a total volume of 20 μ l PCR reaction. The PCR conditions were 94°C for 3 min; 35 cycles of 94°C, 30 sec; 57°C, 30 sec; 72°C, 40 sec; followed by a final extension at 72°C for 7 min. The zebrafish β -actin was used as a control. The PCR product was electrophoresed on a 2% agarose gel and visualized by ethidium bromide staining under UV light.

Recombinant UGT Production. We expressed each of the 40 zebrafish recombinant UGT proteins by subcloning the corresponding cloned cDNA from the pGEM vector into the expression vector pcDNA3 (Huang and Wu, 2010). Briefly, the zebrafish *Ugt* open reading frame from each of the 40 pGEM-T plasmids (Huang and Wu, 2010) was subcloned with primers (Supplemental Table S2) into the expression vector pcDNA3 containing a myc tag, and confirmed by sequencing. It has been shown that the C-terminal tag does not interfere with the glucuronidating activity of the recombinant human UGT protein

MOL #91462

(Zhang et al., 2012). For recombinant zebrafish UGT production, HEK293T cells were transfected at 90% confluency in a 10-cm dish with 12 μ g of experimental or mock plasmids using Lipofectamine 2000. After 6 hrs, the medium was changed. The cells were then grown in the high-glucose Dulbecco's modified Eagle medium (DMEM) supplemented with 10% fetal bovine serum, 4 mM L-glutamine, and 100 μ g/ml penicillin/streptomycin in a humidified incubator with 5% CO₂ at 37°C. The cells were harvested by scraping and washed in a phosphate buffered saline 48 hrs after transfection. The cell suspension was subsequently centrifuged at 500 g for 5 min. The pellet was resuspended with phosphate buffer (0.1 M, pH 7.4) containing dithiothreitol and phenylmethylsulfonyl fluoride. The resuspended cells were lysed by sonication using an ultrasonic processor Uibra cell (Sonics & Materials, USA). 500 μ l suspension of cells was sonicated for four trains each of 5-second bursts, separated by at least 1 min of cooling on ice. Lysates were centrifuged at 12,000 g for 10 min. The supernatant fraction was aliquoted and the aliquots were frozen at -80°C until used. The protein concentration was determined using the Bradford method with bovine serum albumin as the standard.

Western Blot. The relative expression levels of individual recombinant UGT proteins were evaluated using the Western blot analyses. Each of the 40 recombinant zebrafish UGT proteins was separated by 10% SDS-PAGE and transferred onto a nitrocellulose membrane. The membranes were then probed with a mouse anti-myc antibody (Millipore; 1:2,000 dilution) or a mouse anti-actin antibody (Abgent; 1:5,000 dilution). A goat anti-mouse IgG antibody (1:10,000 dilution) conjugated with IR dye 800CW (Biosciences) was subsequently used as the second antibody. The expression of each UGT protein was visualized and quantified using the Odyssey Infrared Imaging system (LI-COR Biosciences, USA).

MOL #91462

Endoglycosidase H (Endo H) Treatment. The supernatant fraction of the cell lysates containing recombinant zebrafish UGT proteins was adjusted to 2 mg/ml with a glycoprotein denaturing buffer, and denatured by heating at 100°C for 10 min. The denatured proteins (10 µg) were incubated with 250 U of Endo H in 50 mM sodium citrate buffer (pH 5.5) at 37°C for 1 hr, and then subjected to 8% SDS-PAGE and Western blot analyses.

Glucuronidation Activity Assay. The glucuronidation assay was performed as previously described (Uchaipichat et al., 2004) with minor modifications. Briefly, 100 µl of the assay mixture contained 0.1 M phosphate buffer (pH 7.4), 5 mM MgCl₂, 200 µg of lysates containing recombinant proteins, and the tested aglycone substrate. The lysate of HEK293T cells transfected with empty vector was used as negative mock controls. After preincubating the assay mixture at 30°C for 3 min in a thermomixer (Eppendorf) with automatic shaking, the reaction was initiated by the addition of 5 mM UDPGA. Incubation was continued for 30-120 min before being terminated by adding 100 µl of ice-cold methanol or acetonitrile. Both incubation times and protein concentrations in the assays were within the linear range of individual UGT activities. After centrifugation at 14,000 g for 5 min, the supernatant was subjected to an HPLC column (COSMOSIL 5C18-AR-II) and analyzed for the presence of glucuronide conjugates in an HPLC machine (Prominence LC-20A from Shimadzu) with a UV or fluorescence detector under the conditions shown in Table 1. The limits of detection of the HPLC assays were determined at signal to noise ratios of 3 (Supplemental Table S3). The identities of the glucuronide conjugates were confirmed by running HPLC with 4-MU-G, 4-NP-G, 1-naphthol-G, E₂-3G, E₂-17G, or with the glucuronidated products using mouse

MOL #91462

liver microsomes with or without UDPGA (data not shown). In particular, the identity of the mono- and di-glucuronidated bilirubin was also confirmed by a validation assay by using the recombinant human UGT1A1 proteins. Finally, the bilirubin glucuronidating activity of the recombinant zebrafish UGT1B7 was confirmed by three control experiments: with mock lysates, without bilirubin, or without UDPGA. The activities were normalized to the relative expression levels of individual UGT proteins with UGT1A1 set as 1.0. All of the glucuronidation reactions were performed at least three times.

For the initial screening of the zebrafish UGT activity, each of the 40 recombinant zebrafish UGT was incubated with one of ten aglycone substrates (500 μ M 4-MU, 2,500 μ M 4-NP, 2,500 μ M 1-naphthol, 200 μ M BPA, 500 μ M t-OP, 1,000 μ M MPA, 500 μ M E₂, 500 μ M testosterone, 150 μ M bilirubin, or 2,500 μ M diclofenac). The glucuronidation assays were performed as described above but with a longer incubation time of 12 hrs. When estradiol, testosterone, bilirubin, bisphenol A, or diclofenac was used as a substrate, DMSO was added to the reaction mixture at a final concentration of 10%. This concentration of DMSO does not inhibit the enzymatic activity.

Kinetic Analysis. For kinetic measurements, we used at least seven different aglycone concentrations and adjusted the enzyme concentration so that no more than 5% of the substrate was consumed during the reactions. In the case of 4-MU, the aglycone concentrations were between 7.5 and 1,000 μ M for UGT1A7; between 2.5 and 150 μ M for UGT1B1. In the case of 4-NP, the aglycone concentrations were between 100 and 10,000 μ M for UGT1A1, between 100 and 5,000 μ M for UGT1A7, and between 50 and 10,000 μ M for UGT1B1. In the case of 1-naphthol, the aglycone concentrations were between 5 and 1,000 μ M for

MOL #91462

UGT1A1, between 2.5 and 150 μM for UGT1B1, and between 150 and 7,500 μM for UGT5A5. In the case of BPA, the aglycone concentrations were between 25 and 500 μM . In the case of t-OP, the aglycone concentrations were between 25 and 1,000 μM for UGT5A5 and between 50 and 1,000 μM for UGT5B2. In the case of MPA, the aglycone concentrations were between 50 and 2,500 μM for UGT1A1 and between 25 and 750 μM for UGT1B1. In the case of E₂, the aglycone concentrations were between 10 and 500 μM for UGT1B1 and between 5 and 250 μM for UGT5E1. In the case of testosterone, the aglycone concentrations were between 10 and 1,000 μM . In the case of diclofenac, the aglycone concentrations were between 50 and 5,000 μM . All of the assays were carried out in duplicates.

The kinetic constants were estimated using nonlinear fitting of experimental data to the following kinetic equations with Graphpad Prism 6.

The Michaelis-Menten equation (eq. 1) (Johnson and Goody, 2011; Michaelis and Menten, 1913):

$$v = \frac{V_{\max} \times [S]}{K_m + [S]} \quad (1)$$

where v is the rate of reaction, V_{\max} is the maximum reaction rate, K_m is the substrate concentration at which the reaction rate is half of V_{\max} , and $[S]$ is the substrate concentration.

The substrate inhibition equation (eq. 2) (Luukkanen et al., 2005):

$$v = \frac{V_{\max} \times [S]}{K_m + [S] + \frac{[S]^2}{K_i}} \quad (2)$$

where K_i is the constant describing the substrate inhibitory potency.

MOL #91462

For data showing both sigmoidal kinetics and substrate inhibition kinetics, the kinetic constants were calculated using a modified Hill equation (eq. 3) (Hill, 1910; LiCata and Allewell, 1997):

$$v = \frac{V_{\max} + V_i \times \left(\frac{[S]}{K_i}\right)^2}{1 + \left(\frac{K_s}{[S]}\right)^n + \left(\frac{[S]}{K_i}\right)^2} \quad (3)$$

where K_s is the dissociation constant of the ES complex, V_i is the reaction rate in the presence of inhibition, and n is the Hill coefficient.

Goodness of fitting to the three equations was evaluated on the basis of standard deviations of the parameter estimates at 95% confidence intervals, and R^2 values, and by visual inspection of the Michaelis-Menten (Johnson and Goody, 2011; Michaelis and Menten, 1913) and Eadie-Hofstee (Eadie, 1942; Hofstee, 1959) plots.

Intrinsic clearance (CL_{int}) was calculated as V_{\max}/K_m for both Michaelis-Menten kinetics and substrate inhibition kinetics. For sigmoidal kinetics, maximum clearance (CL_{max}) was calculated with the following equation (eq. 4) (Houston and Kenworthy, 2000):

$$CL_{\text{max}} = \frac{V_{\max}}{K_s} \times \frac{(n-1)}{n(n-1)^{1/n}} \quad (4)$$

MOL #91462

Results

Tissue-Specific Expression Patterns of the Zebrafish Ugt Gene Repertoire. We recently identified the complete zebrafish *Ugt* gene repertoire and found that the zebrafish genome contains 40 putative functional genes and 5 pseudogenes (Huang and Wu, 2010). To characterize their tissue-specific expression profiles, we measured the expression pattern of each member of the zebrafish *Ugt* superfamily in a wide variety of tissues, including brain, eye, gill, heart, kidney, spleen, liver, intestine, ovary, testis, and muscle, by using an isoform-specific semiquantitative RT-PCR method (Fig. 1, A-C). In addition, quantitative real-time PCR experiments were performed for 8 representative members of the *Ugt* gene superfamily in 4 representative tissues. The results were consistent with those from the isoform-specific semiquantitative RT-PCR assays (Supplemental Fig. S1). The specificity of each primer pair was confirmed by sequencing the amplicons. β -actin was used as an internal control (Fig. 1D).

Ugt1 Clusters. Members of the *Ugt1a* subfamily display distinct tissue-specific expression patterns (Fig. 1A). *Ugt1a1* is highly expressed in the liver, intestine, testis, and spleen, and at low levels in the brain, gill, ovary, and muscle. There are low levels of expression of *Ugt1a2* in the intestine and of *Ugt1a6* in the liver and intestine. *Ugt1a3* and *Ugt1a4* are mainly expressed in the liver, intestine, and testis. In addition, *Ugt1a4* is expressed at low levels in the gill and spleen. *Ugt1a5* is predominantly expressed in the gill, and moderately in the kidney and liver. Finally, *Ugt1a7* is expressed at high levels in the gill and intestine, and at very low levels in the liver, kidney, and testis. Interestingly, none of the *Ugt1a* subfamily is detectable in the eye and heart (Fig. 1A).

MOL #91462

Among members of the *Ugt1b* subfamily, *Ugt1b1* is expressed in all of the tissues examined (Fig. 1A). The expression patterns of *Ugt1b2* to *Ugt1b5* are very similar in the fact that they are mainly expressed in the intestine, liver, and kidney. In addition, *Ugt1b2* is also expressed at low levels in the muscle, and *Ugt1b3* and *Ugt1b4* at low levels in the gill. Finally, *Ugt1b7* is expressed at high levels in the liver and at low levels in the brain, eye, spleen, intestine, testis, and muscle (Fig. 1A).

Ugt2 Clusters. Compared to members of the *Ugt1a* and *Ugt1b* subfamilies, most members of the *Ugt2a* subfamily are expressed in a broad range of tissues except *Ugt2a4*, which is only expressed in the liver (Fig. 1B). In particular, *Ugt2a1*, *Ugt2a3*, and *Ugt2a5* are expressed in all of the tissues examined. Specifically, *Ugt2a1* shows high levels of expression in all tissues except the brain and eye; *Ugt2a3* is highly expressed in the liver and intestine; *Ugt2a5* is expressed at high levels in all tissues. *Ugt2a2* exhibits modest expression in most tissues, including the intestine, liver, ovary, testis, kidney, spleen, and muscle, and low levels in the gill and heart. Finally, *Ugt2a6* is expressed in most tissues except the brain and muscle (Fig. 1B).

Members of the *Ugt2b* subfamily are expressed at high levels in the liver and intestine except *Ugt2b6* (Fig. 1B). In addition, *Ugt2b1* is also expressed in the spleen and at low levels in the testis and kidney. *Ugt2b3* shows low levels of expression in the testis. *Ugt2b5* is expressed with high levels in the kidney and testis, and low levels in the gill and spleen. Finally, *Ugt2b6* is expressed at low levels in the heart, spleen, liver, ovary, and testis (Fig. 1B).

MOL #91462

Ugt5 Clusters. The *Ugt5* genes encode a novel family of UDP glucuronosyltransferases that have distinct genomic organization and only exist in lower vertebrates (Huang and Wu, 2010). For members of the *Ugt5a* cluster, *Ugt5a1* and *Ugt5a2* display similar expression profiles (Fig. 1C). In addition to high levels of expression in the liver and intestine, *Ugt5a1* and *Ugt5a2* are also expressed at low levels in the eye, gill, kidney, spleen, and testis. *Ugt5a3* is only expressed at low levels in the liver and intestine (Fig. 1C). *Ugt5a4* is expressed at high levels in the liver and intestine, and at low levels in the gill and testis. *Ugt5a5*, the most ancient gene in the cluster (Huang and Wu, 2010), is ubiquitously expressed in all tissues (Fig. 1C).

Both *Ugt5b1* and *Ugt5b2* have two alternative upstream 5' noncoding exons (*u1* and *u2*) and alternative splicing from these two noncoding exons generate two variants for each of *Ugt5b1* and *Ugt5b2* (Fig. 1C) (Huang and Wu, 2010). Interestingly, we found that the two variants of *Ugt5b1* and *Ugt5b2* have different expression patterns. The *u1* variant of *Ugt5b1* is expressed at high levels in the gill and spleen, and at low levels in the heart, kidney, liver, intestine, ovary, and testis. The *u2* variant of *Ugt5b1* is expressed at high levels in the gill, kidney, and spleen, and at low levels in the liver, intestine, ovary, and muscle (Fig. 1C). The *u1* variant of *Ugt5b2* is expressed at high levels in all of the tissues except the heart. The *u2* variant of *Ugt5b2* is expressed at high levels in the eye, gill, and kidney, but at low levels in the ovary (Fig. 1C). This observation suggests that the two upstream noncoding exons were differentially spliced in a tissue-specific manner. The expression of *Ugt5b3* is limited to the intestine and liver, with a higher level in the intestine. Finally, *Ugt5b4* is expressed at high levels in the brain, eye, gill, kidney, spleen, liver, and intestine, and at low levels in the testis (Fig. 1C).

MOL #91462

There are three members of the *Ugt5c* cluster (Huang and Wu, 2010). *Ugt5c1* is expressed at low levels in the brain, spleen, intestine, and testis (Fig. 1C). *Ugt5c2* is expressed at high levels in the kidney, spleen, liver, intestine, and ovary, and at low levels in the eye and testis (Fig. 1C). Finally, *Ugt5c3* is highly expressed in all tissues except in the gill (Fig. 1C).

Other members of the *Ugt5* family, including *Ugt5d1*, *Ugt5e1*, *Ugt5f1*, *Ugt5g1*, and *Ugt5g2*, are non-clustered *Ugt* genes (Huang and Wu, 2010). *Ugt5d1* is expressed at high levels in the liver and intestine, and at low levels in the spleen, testis, and ovary (Fig. 1C). *Ugt5e1* is expressed in the eye, gill, heart, kidney, and testis (Fig. 1C). *Ugt5f1* and *Ugt5g1* are ubiquitously expressed in all tissues except the eye and spleen (Fig. 1C). Interestingly, *Ugt5g2* is only expressed at high levels in the eye and at low levels in the gill (Fig. 1C).

Glucuronidation Activities of the Zebrafish UGT Superfamily Proteins. Although glucuronidation is known to be an important pathway in fish species, to date no member of the zebrafish UGT superfamily has been shown to have catalytic glucuronidating activity (Dutton, 1980; James, 2011). To investigate the biological function of individual members of the UGT superfamily in zebrafish, we expressed each of the 40 recombinant UGT proteins in HEK293T cells. We confirmed the expression of recombinant proteins using Western blot analysis (Fig. 2A). Interestingly, we observed multiple bands for most UGT isoforms; however, treatment of individual UGTs with Endoglycosidase H (Endo H) invariably resulted in a single polypeptide band (Fig. 2B). This demonstrated that the multiple bands are derived from different levels of

MOL #91462

the glycosylation of the same UGT enzyme.

We measured the glucuronidation activities of the zebrafish UGT enzymes, with UDP-glucuronic acid as the donor, toward ten commonly used aglycone substrates, including three small phenols (4-MU, 4-NP, 1-naphthol), three complex phenols (BPA, t-OP, and MPA), two hormone steroids (E₂ and testosterone), and two carboxylic acids (bilirubin and diclofenac) (Table 2) by using the HPLC system to separate the conjugated glucuronide from the respective aglycone substrate (Fig. 3 and 4). The substrate (aglycone) concentrations used to obtain the data shown in Table 2 were the same as that used in the initial screening (see the method section). The HPLC chromatograms of glucuronidation assays with members of the UGT1 and UGT2 families were shown in Fig. 3 for enzymes with strong activities toward specific substrates and in the Supplemental Figure S2 for the others. The results for UGT5 were shown in Fig. 4.

UGT1 Family. Some members of the UGT1 family have strong glucuronidation activities toward most of the phenols (except t-OP) and carboxylic acids (Table 2; Fig. 3 and S2). Moreover, UGT1 is the only family with isoforms that can conjugate bilirubin and BPA. However, no member of the UGT1 family can glucuronidate steroids (Table 2; Fig. 3 and S2), except UGT1A1 and UGT1B1, which have trace glucuronidation activities toward β -estradiol at the 3'-OH position (Table 2; Fig. S2D and 3I).

Among the seven members of the UGT1A subfamily, UGT1A1 glucuronidates most of the substrates except testosterone (Table 2), and is the most active isozyme involved in the glucuronidation of 1-naphthol (Fig. 3A), BPA (Fig. 3B), MPA (Fig. 3C), and diclofenac (Fig. 3D). Multiple peaks appeared in the HPLC

MOL #91462

chromatogram after diclofenac was conjugated by recombinant zebrafish UGTs, probably due to the intramolecular rearrangement of acyl-glucuronides (Harada et al., 2009). Moreover, UGT1A1 also has glucuronidation activities toward the coumarin derivative 4-MU (Fig. S2A), the small phenol 4-NP (Fig. S2B), complex phenol t-OP (Fig. S2C), steroid E₂ (Fig. S2D), and endobiotic bilirubin (Fig. S2E). UGT1A3 has high glucuronidation activity toward MPA (Fig. 3E) and low activity toward 4-MU (Fig. S2F), 4-NP (Fig. S2G), 1-naphthol (Fig. S2H), BPA (Fig. S2I), t-OP (Fig. S2J), bilirubin (Fig. S2K), and diclofenac (Fig. S2L). UGT1A4 has a low activity toward 4-MU (Fig. 3F) and trace activities toward 4-NP (Fig. S2M) and 1-naphthol (Fig. S2N). Finally, UGT1A7 has strong activities toward 4-MU (Fig. 3G) and 4-NP (Fig. S2O) and weak activity toward 1-naphthol (Fig. S2P). Its activity toward 4-MU is the highest among all zebrafish UGTs (Table 2).

Among the six members of the UGT1B subfamily, UGT1B1 has glucuronidation activities toward 4-MU (Fig. S2Q), 4-NP (Fig. 3H), 1-naphthol (Fig. S2R), BPA (Fig. S2S), t-OP (Fig. S2T), MPA (Fig. S2U), E₂ (Fig. 3I), and bilirubin (Fig. S2V). In particular, UGT1B1 has high activities toward multiple phenols, including 4-MU, 4-NP, 1-naphthol, and MPA, with its activity toward 4-NP the highest among the 40 zebrafish UGT isozymes (Table 2); however, its activities toward E₂ (3'-OH) and t-OP are very low (Table 2). Interestingly, UGT1B1 and two members of UGT1A (1A1 and 1A3) conjugate a common set of aglycone substrates, including all of the six phenols as well as bilirubin (Table 2), consistent with the fact that these three genes are close paralogs (Huang and Wu, 2010). UGT1B2 has trace activities toward three phenols 4-MU (Fig. S2W), 4-NP (Fig. S2X), and 1-naphthol (Fig. S2Y). Finally, UGT1B7 glucuronidates bilirubin at the highest rate among all of the zebrafish UGTs, suggesting its important role in bilirubin

MOL #91462

metabolism (Table 2; Fig. 3J).

UGT2 Family. Among members of the UGT2 family, we found that UGT2B3 has low glucuronidation activities toward three phenols 4-MU (Fig. S2Z), 4-NP (Fig. S2AA), and 1-naphthol (Fig. 3K). Moreover, UGT2B6 has low glucuronidation activities toward 4-MU (Fig. 3L), 4-NP (Fig. S2AB), and 1-naphthol (Fig. S2AC). Other members of the UGT2 family do not have detectable glucuronidation activity toward the ten substrates examined.

UGT5 Family. In contrast to the variable and constant genomic organization of the *Ugt1* and *Ugt2* families, the zebrafish *Ugt5* genes form a novel family with strikingly distinct genomic organization. The entire open reading frame of each *Ugt5* gene (except *Ugt5g2*) is encoded by a single large exon (Huang and Wu, 2010). In addition, they are the most abundant *Ugt* genes in teleosts. Among the seventeen zebrafish UGT5s, we found that UGT5A4, UGT5A5, UGT5B2, UGT5C3, and UGT5E1 have glucuronidation activities toward at least one of the ten substrates (Fig. 4). None of the UGT5s is capable of glucuronidating BPA and bilirubin (Table 2).

We found that UGT5A4 has very low glucuronidation activity toward t-OP (Fig. 4A). We detected a small peak of the conjugated substrate t-OP-G for the recombinant UGT5A4 but not the mock in the HPLC chromatograms (see the inset in Fig. 4A). In addition, this small peak disappeared when the donor UDPGA was opted out of the glucuronidation assay (data not shown). Thus, UGT5A4 has low but definitive glucuronidation activity toward t-OP.

MOL #91462

UGT5A5, the most ancient (Huang and Wu, 2010) and ubiquitously expressed member of the UGT5A subfamily (Fig. 1C), is capable of conjugating phenols, steroids, and carboxylic acids, including 4-MU (Fig. 4B), 4-NP (Fig. 4C), 1-naphthol (Fig. 4D), t-OP (Fig. 4E), MPA (Fig. 4F), E₂ (Fig. 4G), testosterone (Fig. 4H), and diclofenac (Fig. 4I). We noted that, when E₂ was used as an aglycone substrate, two glucuronide peaks appeared (Fig. 4G). We confirmed that these two peaks corresponded to E₂-3-G and E₂-17-G, respectively, by running HPLC with commercial E₂-3-G and E₂-17-G as the standards (data not shown). The rate of glucuronidation at E₂ (17'-OH) is much higher than at E₂ (3'-OH), suggesting its preference for the 17'-OH position of steroids (Fig. 4G). As expected, UGT5A5 also glucuronidates the steroid of testosterone at the corresponding position (17'-OH) (Fig. 4H).

For members of the UGT5B subfamily, we found that UGT5B2 is capable of conjugating 4-MU (Fig. 4J), 4-NP (Fig. 4K), 1-naphthol (Fig. 4L), t-OP (Fig. 4M), and E₂ (3'-OH) (Fig. 4N). Its activities toward t-OP and E₂ (3'-OH) are the highest among all of the zebrafish UGTs (Table 2). Among members of the UGT5C subfamily, only UGT5C3 conjugates 4-MU (Fig. 4O) and t-OP (Fig. 4P).

Among the five members of the nonclustered *Ugt5* genes, the extrahepatic UGT5E1 glucuronidates 4-MU (Fig. 4Q), 4-NP (Fig. 4R), and t-OP (Fig. 4S) at relatively low rates; however, its activities toward the 17'-OH position of E₂ (Fig. 4T) and testosterone (Fig. 4U) are the highest among all of the zebrafish UGTs, suggesting its important role in metabolizing these two sex hormones.

MOL #91462

Kinetic Analyses. To further investigate the enzymatic properties of the zebrafish UGTs, kinetic analyses were carried out for six UGT isoforms with high glucuronidation activity. These isoforms include three members each of UGT1 and UGT5 families (Table 3). We performed a series of glucuronidation assays with various concentrations of aglycone substrates, and fitted the experimental data to the appropriate equations (Fig. 5).

At high concentrations of aglycones, substrate inhibition was observed for all six UGT isoforms with the exception of t-OP for UGT5A5 (Fig. 5). This may be a phenomenon of the mammalian expression system.

A mechanism based on the nonproductive accumulation of a dead-end ternary complex (enzyme-UDP-substrate) has been proposed to explain the substrate inhibition phenomena of glucuronidation reactions (Luukkanen et al., 2005). Our substrate inhibition data fitted well to the substrate inhibition equation (eq. 2) (Table 3; $R^2 = 0.9631 \sim 0.9992$) (Fig. 5, A-H, J-L, and O-Q). The conjugation of 4-NP by UGT1B1 and 1-Naphthol by UGT5A5 showed both substrate inhibition and sigmoidal kinetics (Fig. 5, I and M) and the data fitted well to a modified Hill equation (eq. 3) (Table 3; $R^2 = 0.9959$ and 0.9987 , respectively). In the case of t-OP for UGT5A5, the relatively low catalytic capacity of UGT5A5 (Tables 2 and 3) and low solubility of t-OP prevented us from observing the substrate inhibition. However, the data fitted very well to the Michaelis-Menten equation (eq. 1) (Table 3; $R^2 = 0.9992$) (Fig. 5N). The corresponding glucuronidation kinetic parameters were calculated from the appropriate models and listed in Table 3.

UGT1 Family. UGT1A1 displays comparably high turnover rates (V_{max}) toward 4-NP, 1-naphthol, MPA,

MOL #91462

and diclofenac (Table 3). However, the apparent K_m values for 1-naphthol and MPA are about one order of magnitude lower than those for 4-NP and diclofenac. Thus, UGT1A1 has higher affinity and glucuronidation efficiency (CL_{int}) toward 1-naphthol and MPA (Table 3). Although UGT1A1 is the isozyme with the highest activity among all of the zebrafish UGTs toward BPA (Table 2), its efficiency toward BPA is lower than that toward 1-Naphthol and MPA (Table 3).

UGT1A7 conjugates 4-MU ($CL_{int} = 6.01$) more efficiently than 4-NP ($CL_{int} = 0.62$). Its catalytic efficiency toward 4-NP is comparable to that of UGT1A1. For both UGT1A1 and UGT1A7 catalyzed reactions, substrate inhibition was not significant ($K_i \gg K_m$) (Table 3).

UGT1B1 is the most efficient (CL_{int} or CL_{max}) isoform for phenolic aglycone glucuronidation (Table 3). This may be partly due to its high affinity toward phenolic compounds. Its apparent K_m values for phenolic aglycones (4-MU, 4-NP, 1-naphthol, and MPA) are much lower than those of the other isoforms (Table 3). In conjunction with its high-level expression in multiple tissues (Fig. 1A), these data suggest an important role of UGT1B1 in *in-vivo* detoxification of phenolic compounds. Strikingly, 4-NP glucuronidation by UGT1B1 showed significant substrate inhibition and autoactivation (Table 3, Hill coefficient = 1.75), which was also reported for several human UGTs (Uchaipichat et al., 2008). In contrast to its high efficiency toward phenolic aglycones, UGT1B1 conjugates the steroid hormone E_2 at very low efficiency, with a CL_{int} value of 0.094, which is about 2 orders of magnitude lower than that for phenolic aglycones (Table 3). The substrate inhibition for UGT1B1 is also not significant as suggested by the high ratio of K_i/K_m .

MOL #91462

UGT5 Family. Although UGT5A5 displays the broadest substrate spectrum toward the ten aglycones (Table 2; Fig. 4, B-I), its glucuronidation efficiency toward 1-naphthol and t-OP is very low (1-naphthol $CL_{\max} = 0.0017$ and t-OP $CL_{\text{int}} = 0.0084$) (Table 3). Its glucuronidation toward 1-naphthol also showed both substrate inhibition and sigmoidal kinetics, with a Hill value of 1.11. Furthermore, the K_i value of UGT5A5 toward 1-naphthol is much lower than the K_s value, suggesting a high substrate inhibition.

UGT5B2 conjugates t-OP much more efficiently and at a higher turnover rate than UGT5A5, with values of clearance and V_{\max} two orders of magnitude higher (Table 3). It also shows a strong substrate inhibition ($K_i < K_m$).

UGT5E1 displays not only the highest turnover rate but also the highest affinity for 17'-OH of E_2 and testosterone, with K_m values of 13.4 and 30.6 μM , respectively (Table 3). This suggests that UGT5E1 plays an important role in the homeostasis of these two steroid hormones *in vivo*. Finally, the substrate inhibition for these reactions is very weak ($K_i/K_m > 100$).

In summary, our kinetic analyses demonstrate that diverse UGT enzymes have distinct affinity and glucuronidation efficiency toward various aglycone substrates.

MOL #91462

Discussion

The genomic organization of the mammalian *Pcdh* and *Ugt1* gene clusters is strikingly similar in that both contain a tandem array of highly-similar variable exons followed by a common set of downstream constant exons (Zhang et al., 2004). In contrast to the cell-specific expression of *Pcdh* genes in the brain, members of the mouse *Ugt1* cluster display tissue-specific expression patterns in a wide variety of tissues, especially in the digestive and respiratory systems (Zhang et al., 2004). In addition, the variable and constant genomic organizations of both the *Pcdh* and *Ugt1* clusters are conserved in zebrafish (Li and Wu, 2007; Wu, 2005). The zebrafish has become an important vertebrate model organism for developmental biology, physiology, and pathology studies (Howe et al., 2013). Recently, there has been great interest in developing the zebrafish as a vertebrate model organism for drug discovery as well as for environmental toxicology (Hill et al., 2005; Peterson and Macrae, 2012). The full complement of the phase I drug-metabolizing cytochrome P450 genes has been identified in zebrafish (Goldstone et al., 2010). We recently identified the complete repertoire of the zebrafish phase II drug-metabolizing *Ugt* gene superfamily and found that they are divided into three families, *Ugt1*, *Ugt2*, and *Ugt5* (Huang and Wu, 2010). These zebrafish *Ugt* genes do not display orthologous relationships to any of the mammalian or avian *Ugts*, making it difficult to predict their substrate specificities. Here, we report the tissue-specific expression patterns of the complete zebrafish *Ugt* repertoire. We also systematically analyzed their substrate specificity and glucuronidation activity toward ten aglycone substrates and found that most zebrafish UGTs are true glucuronidating enzymes with UDPGA as the donor.

To develop the zebrafish as a model organism for toxicology screening in the drug discovery pipeline,

MOL #91462

elucidating the mechanisms by which drug-metabolizing enzymes conjugate aglycone substrates is an important prerequisite (Peterson and Macrae, 2012). Moreover, large efforts have been undertaken to develop the zebrafish as a sentinel model organism for environmental toxicants and agents (Carvan et al., 2000; James, 2011). It is vital to systematically characterize the expression profiles as well as the catalytic functions of the complete zebrafish *Ugt* repertoire. Expression profiling analyses revealed that members of the zebrafish *Ugt* superfamily are expressed in a tissue-specific manner. For example, *Ugt1a2*, *Ugt1a5*, *Ugt2a4*, and *Ugt5g2* appear to be specifically expressed in the intestine, gill, liver, and eye, respectively. In addition, several *Ugt* genes (*Ugt1b5*, *Ugt1a7*, *Ugt2b3*, *Ugt5a3*, and *Ugt5b3*) are only expressed in two to three organs, suggesting that they play important roles in organ-specific toxicity.

Interestingly, multiple zebrafish *Ugt* genes, especially members of the *Ugt1a*, *Ugt2a*, *Ugt5b*, *Ugt5e*, *Ugt5f*, and *Ugt5g* subfamilies, are expressed in the gill which is the respiratory organ that interacts directly with the xenobiotics in the aquatic environment. These *Ugt* genes may be important in metabolizing large numbers of chemical agents from the aquatic environment. In the kidney, most members of the *Ugt2* and *Ugt5* families are highly expressed, while most members of the *Ugt1* family are expressed at low levels. In particular, *Ugt5e1* is enriched in the testis and gill, and it has the highest glucuronidation efficiency toward hormone steroids (E_2 and testosterone, Table 3) as demonstrated by functional analyses. The steroid glucuronides have been reported to serve as sex pheromones capable of inducing ovulation or attracting opposite sex (Van den Hurk et al., 1987). To investigate the functional significance of the tissue-specific expression patterns of the *Ugt* repertoire, we systematically characterized the catalytic activities of the encoded enzymes by expressing each of the 40 recombinant UGTs and then testing them with ten

MOL #91462

aglycone substrates in a glucuronidation assay with UDPGA as the donor. Interestingly, we found that many of the recombinant zebrafish UGTs are N-glycosylated in HEK293T cells. The glycosylation of zebrafish UGTs might affect their enzymatic activity or substrate specificity.

We found that zebrafish UGT1A1, UGT1A3, and UGT1B1 have high glucuronidation activity toward six important phenolic aglycone substrates: 4-MU, 4-NP, 1-naphthol, BPA, t-OP, and MPA. 4-MU, a coumarin derivative, has been used safely for many years as a cholagogue and is a promising therapeutic agent targeting invasion and metastasis of many kinds of tumors via inhibition of hyaluronan synthesis (Kakizaki et al., 2004). 4-NP is a common metabolite from a variety of compounds and a biomarker of organophosphate insecticide exposure (Kaivosaaari et al., 2011). 1-Naphthol, a prime substrate for human UGT1A6, is a precursor to a variety of insecticides and a prominent component of Molisch's reagent. BPA is a monomer for manufacturing polycarbonate plastics and epoxy resins and can be released during autoclaving. It has hormone-like activities which disrupt the endocrine system and increase the risk of obesity (Howdeshell et al., 1999). Among environmental alkylphenols, t-OP is the most estrogenic (Routledge and Sumpter, 1997). MPA is the active metabolite of mycophenolate mofetil, a prodrug used to prevent tissue rejection after organ transplantation (Wu et al., 2011).

Steroid hormones are mainly metabolized via glucuronidation (James, 2011). In human, steroid hormones are predominantly glucuronidated by members of the UGT2 family (Sten et al., 2009). In zebrafish, however, they are mainly conjugated by members of the UGT5 family (Tables 2 and 3). UGT5E1 is the principal enzyme responsible for steroid conjugations, with high activity and affinity toward testosterone

MOL #91462

and E₂. The *Ugt5e1* gene is expressed in the extrahepatic tissues of the gill, heart, kidney, testis, and eye (Fig. 1C).

Bilirubin, a major breakdown product of heme catabolism, is excreted predominantly as glucuronide conjugates in the bile. In zebrafish, we found that it is conjugated by several UGT1 enzymes at very low rates. Among them, UGT1B7 has the highest glucuronidation activity toward bilirubin, mainly forming the monoglucuronides (Fig. 3J). In addition, we found that UGT1B7 is specific toward bilirubin, with no detectable glucuronidation activity toward any of the other nine aglycone substrates. Moreover, the *Ugt1b7* gene is highly expressed in the liver, which is responsible for bilirubin catabolism.

Diclofenac, a nonsteroidal anti-inflammatory drug widely used for reducing inflammation and relieving pain, is primarily eliminated as acyl-glucuronide in mammals (King et al., 2001). Its acyl-glucuronide forms covalent drug-protein adducts, possibly contributing to its immunogenicity and toxicity (King et al., 2001). In zebrafish, UGT1A1 is the only isozyme that has a high rate of diclofenac glucuronidation (Table 2). However, kinetic analyses revealed a very high K_m value of UGT1A1 for diclofenac, indicating its low affinity.

In summary, members of the zebrafish *Ugt* superfamily are widely expressed in various tissues. In addition, some members of the zebrafish UGT5 family have glucuronidation activities toward multiple aglycones. Specifically, the zebrafish UGT5A5 and UGT5E1 predominantly glucuronidate the hormone steroids of E₂ and testosterone, and the zebrafish UGT5B2 glucuronidates t-OP at the highest rate and

MOL #91462

several phenols at a lower rate. Thus, UGT5 is a novel UGT family using UDPGA as the donor. Moreover, some members of the zebrafish UGT1 family conjugate a wide range of compounds, including simple phenols, bilirubin, carboxylic acids, coumarins, mycophenolic acid, and bisphenol A. Importantly, each of these lipophilic compounds is conjugated by at least one member of the UGT superfamily, confirming that these diverse 40 UGTs are the entire complement of the zebrafish phase II glucuronosyltransferases. These results provide insight into the mechanisms by which zebrafish defend themselves against a vast number of endobiotics and xenobiotics via glucuronidation conjugations, and lay the foundation for developing the zebrafish as a model vertebrate in toxicological, developmental and pathological studies.

MOL #91462

Acknowledgments

We thank Dr. Ida Owens for her advice on investigating UGT posttranslational modification and members of the Wu lab for discussion.

Authorship contributions

Participated in research design: Wang, Huang, and Wu.

Conducted experiments: Wang and Huang.

Performed data analysis: Wang, Huang, and Wu.

Wrote or contributed to the writing of the manuscript: Wang, Huang, and Wu.

MOL #91462

References

Carvan MJ, 3rd, Dalton TP, Stuart GW, and Nebert DW (2000) Transgenic zebrafish as sentinels for aquatic pollution.

Ann N Y Acad Sci **919**: 133-147.

Clarke DJ, Burchell B, and George SG (1992) Functional and immunochemical comparison of hepatic

UDP-glucuronosyltransferases in a piscine and a mammalian species. *Comp Biochem Physiol B* **102**: 425-432.

Dutton GJ (1980) *Glucuronidation of Drugs and Other Compounds*. CRC Press, Boca Raton, FL.

Eadie GS (1942) The Inhibition of Cholinesterase by Physostigmine and Prostigmine. *J Biol Chem* **146**: 85-93.

Emi Y, Ikushiro S, and Iyanagi T (1995) Drug-responsive and tissue-specific alternative expression of multiple first

exons in rat UDP-glucuronosyltransferase family 1 (UGT1) gene complex. *J Biochem (Tokyo)* **117**: 392-399.

Goldstone JV, McArthur AG, Kubota A, Zanette J, Parente T, Jönsson ME, Nelson DR, and Stegeman JJ (2010)

Identification and developmental expression of the full complement of Cytochrome P450 genes in Zebrafish.

BMC Genomics **11**: 643.

Harada H, Endo T, Momose Y, and Kusama H (2009) A liquid chromatography/tandem mass spectrometry method

for detecting UGT-mediated bioactivation of drugs as their N-acetylcysteine adducts in human liver microsomes.

Rapid Commun Mass Spectrom **23**: 564-570.

Hill AJ, Teraoka H, Heideman W, and Peterson RE (2005) Zebrafish as a model vertebrate for investigating chemical

toxicity. *Toxicological sciences* **86**: 6-19.

Hill AV (1910) The possible effects of the aggregation of the molecules of haemoglobin on its dissociation curves. *J*

Physiol **40 (Suppl)**: 4-7.

Hofstee BH (1959) Non-inverted versus inverted plots in enzyme kinetics. *Nature* **184**: 1296-1298.

Houston JB and Kenworthy KE (2000) In vitro-in vivo scaling of CYP kinetic data not consistent with the classical

MOL #91462

Michaelis-Menten model. *Drug Metab Dispos* **28**: 246-254.

Howdeshell KL, Hotchkiss AK, Thayer KA, Vandenberg JG, and vom Saal FS (1999) Exposure to bisphenol A advances puberty. *Nature* **401**: 763-764.

Howe K, Clark MD, Torroja CF, Torrance J, Berthelot C, Muffato M, Collins JE, Humphray S, McLaren K, Matthews L, McLaren S, Sealy I, Caccamo M, Churcher C, Scott C, Barrett JC, Koch R, Rauch GJ, White S, Chow W, Kilian B, Quintais LT, Guerra-Assunção JA, Zhou Y, Gu Y, Yen J, Vogel JH, Eyre T, Redmond S, Banerjee R, Chi J, Fu B, Langley E, Maguire SF, Laird GK, Lloyd D, Kenyon E, Donaldson S, Sehra H, Almeida-King J, Loveland J, Trevanion S, Jones M, Quail M, Willey D, Hunt A, Burton J, Sims S, McLay K, Plumb B, Davis J, Clee C, Oliver K, Clark R, Riddle C, Elliott D, Threadgold G, Harden G, Ware D, Mortimer B, Kerry G, Heath P, Phillimore B, Tracey A, Corby N, Dunn M, Johnson C, Wood J, Clark S, Pelan S, Griffiths G, Smith M, Glithero R, Howden P, Barker N, Stevens C, Harley J, Holt K, Panagiotidis G, Lovell J, Beasley H, Henderson C, Gordon D, Auger K, Wright D, Collins J, Raisen C, Dyer L, Leung K, Robertson L, Ambridge K, Leongamornlert D, McGuire S, Gilderthorp R, Griffiths C, Manthavadi D, Nichol S, Barker G, Whitehead S, Kay M, Brown J, Murnane C, Gray E, Humphries M, Sycamore N, Barker D, Saunders D, Wallis J, Babbage A, Hammond S, Mashreghi-Mohammadi M, Barr L, Martin S, Wray P, Ellington A, Matthews N, Ellwood M, Woodmansey R, Clark G, Cooper J, Tromans A, Grafham D, Skuce C, Pandian R, Andrews R, Harrison E, Kimberley A, Garnett J, Fosker N, Hall R, Garner P, Kelly D, Bird C, Palmer S, Gehring I, Berger A, Dooley CM, Ersan-Ürün Z, Eser C, Geiger H, Geisler M, Karotki L, Kirn A, Konantz J, Konantz M, Oberländer M, Rudolph-Geiger S, Teucke M, Osoegawa K, Zhu B, Rapp A, Widaa S, Langford C, Yang F, Carter NP, Harrow J, Ning Z, Herrero J, Searle SM, Enright A, Geisler R, Plasterk RH, Lee C, Westerfield M, de Jong PJ, Zon LI, Postlethwait JH, Nüsslein-Volhard C, Hubbard TJ, Roest Crollius H, Rogers J, and Stemple DL (2013) The

MOL #91462

- zebrafish reference genome sequence and its relationship to the human genome. *Nature* **496**: 498-503.
- Huang H and Wu Q (2010) Cloning and comparative analyses of the zebrafish Ugt repertoire reveal its evolutionary diversity. *PLoS One* **5**: e9144.
- James MO (2011) Steroid catabolism in marine and freshwater fish. *J Steroid Biochem Mol Biol* **127**: 167-175.
- Johnson KA and Goody RS (2011) The original Michaelis constant: translation of the 1913 Michaelis-Menten paper. *Biochemistry* **50**: 8264-8269.
- Kaivosaaari S, Finel M, and Koskinen M (2011) N-glucuronidation of drugs and other xenobiotics by human and animal UDP-glucuronosyltransferases. *Xenobiotica* **41**: 652-669.
- Kakizaki I, Kojima K, Takagaki K, Endo M, Kannagi R, Ito M, Maruo Y, Sato H, Yasuda T, Mita S, Kimata K, and Itano N (2004) A novel mechanism for the inhibition of hyaluronan biosynthesis by 4-methylumbelliferone. *J Biol Chem* **279**: 33281-33289.
- King C, Tang W, Ngui J, Tephly T, and Braun M (2001) Characterization of rat and human UDP-glucuronosyltransferases responsible for the in vitro glucuronidation of diclofenac. *Toxicol Sci* **61**: 49-53.
- Li C and Wu Q (2007) Adaptive evolution of multiple-variable exons and structural diversity of drug-metabolizing enzymes. *BMC Evol Biol* **7**: 69.
- LiCata VJ and Allewell NM (1997) Is substrate inhibition a consequence of allostery in aspartate transcarbamylase? *Biophys Chem* **64**: 225-234.
- Luukkanen L, Taskinen J, Kurkela M, Kostianen R, Hirvonen J, and Finel M (2005) Kinetic characterization of the 1A subfamily of recombinant human UDP-glucuronosyltransferases. *Drug Metab Dispos* **33**: 1017-1026.
- Mackenzie PI, Walter Bock K, Burchell B, Guillemette C, Ikushiro S, Iyanagi T, Miners JO, Owens IS, and Nebert DW (2005) Nomenclature update for the mammalian UDP glycosyltransferase (UGT) gene superfamily.

MOL #91462

Pharmacogenet Genomics **15**: 677-685.

Maitland ML, Grimsley C, Kuttub-Boulos H, Witonsky D, Kasza KE, Yang L, Roe BA, and Di Rienzo A (2006)

Comparative genomics analysis of human sequence variation in the UGT1A gene cluster. *Pharmacogenomics J* **6**: 52-62.

Meech R, Miners JO, Lewis BC, and Mackenzie PI (2012) The glycosidation of xenobiotics and endogenous compounds: versatility and redundancy in the UDP glycosyltransferase superfamily. *Pharmacol Ther* **134**: 200-218.

Ménard V, Girard H, Harvey M, Pérusse L, and Guillemette C (2009) Analysis of inherited genetic variations at the UGT1 locus in the French-Canadian population. *Hum Mutat* **30**: 677-687.

Michaelis L and Menten ML (1913) Die Kinetik der Invertinwirkung. *Biochem Z* **49**: 333-369.

Owens IS, Basu NK, and Banerjee R (2005) UDP-glucuronosyltransferases: gene structures of UGT1 and UGT2 families. *Methods Enzymol* **400**: 1-22.

Peterson RT and Macrae CA (2012) Systematic approaches to toxicology in the zebrafish. *Annu Rev Pharmacol Toxicol* **52**: 433-453.

Ritter JK, Crawford JM, and Owens IS (1991) Cloning of two human liver bilirubin UDP-glucuronosyltransferase cDNAs with expression in COS-1 cells. *J Biol Chem* **266**: 1043-1047.

Routledge EJ and Sumpter JP (1997) Structural features of alkylphenolic chemicals associated with estrogenic activity. *J Biol Chem* **272**: 3280-3288.

Saeki M, Saito Y, Jinno H, Sai K, Ozawa S, Kurose K, Kaniwa N, Komamura K, Kotake T, Morishita H, Kamakura S, Kitakaze M, Tomoike H, Shirao K, Tamura T, Yamamoto N, Kunitoh H, Hamaguchi T, Yoshida T, Kubota K, Ohtsu A, Muto M, Minami H, Saijo N, Kamatani N, and Sawada JI (2006) Haplotype structures of the UGT1A

MOL #91462

gene complex in a Japanese population. *Pharmacogenomics J* **6**: 63-75.

Stegeman JJ, Goldstone JV, and Hahn ME (2010) Perspectives on zebrafish as a model in environmental toxicology, in *Zebrafish* (Steve F. Perry ME, Anthony P. Farrell and Colin J. Brauner ed) pp 367-439, Academic Press, Amsterdam.

Sten T, Bichlmaier I, Kuuranne T, Leinonen A, Yli-Kauhaluoma J, and Finel M (2009) UDP-glucuronosyltransferases (UGTs) 2B7 and UGT2B17 display converse specificity in testosterone and epitestosterone glucuronidation, whereas UGT2A1 conjugates both androgens similarly. *Drug Metab Dispos* **37**: 417-423.

Thomas SS, Li SS, Lampe JW, Potter JD, and Bigler J (2006) Genetic variability, haplotypes, and htSNPs for exons 1 at the human UGT1A locus. *Hum Mutat* **27**: 717.

Tokarz J, Möller G, Hrabě de Angelis M, and Adamski J (2013) Zebrafish and steroids: What do we know and what do we need to know? *J Steroid Biochem Mol Biol* **137**: 165-173.

Uchaipichat V, Galetin A, Houston JB, Mackenzie PI, Williams JA, and Miners JO (2008) Kinetic modeling of the interactions between 4-methylumbelliferone, 1-naphthol, and zidovudine glucuronidation by udp-glucuronosyltransferase 2B7 (UGT2B7) provides evidence for multiple substrate binding and effector sites. *Mol Pharmacol* **74**: 1152-1162.

Uchaipichat V, Mackenzie PI, Guo XH, Gardner-Stephen D, Galetin A, Houston JB, and Miners JO (2004) Human UDP-glucuronosyltransferases: isoform selectivity and kinetics of 4-methylumbelliferone and 1-naphthol glucuronidation, effects of organic solvents, and inhibition by diclofenac and probenecid. *Drug Metab Dispos* **32**: 413-423.

Van den Hurk R, Schoonen WGEJ, van Zoelen GA, Lambert JGD (1987) The biosynthesis of steroid glucuronides in

MOL #91462

the testis of the zebrafish, *Brachydanio rerio*, and their pheromonal function as ovulation inducers. *Gen Comp Endocrinol* **68**: 179–188.

Wu B, Kulkarni K, Basu S, Zhang S, and Hu M (2011) First-pass metabolism via UDP-glucuronosyltransferase: a barrier to oral bioavailability of phenolics. *J Pharm Sci* **100**: 3655-3681.

Wu Q (2005) Comparative genomics and diversifying selection of the clustered vertebrate protocadherin genes. *Genetics* **169**: 2179-2188.

Yang J, Cai L, Huang H, Liu B, and Wu Q (2012) Genetic variations and haplotype diversity of the UGT1 gene cluster in the Chinese population. *PLoS One* **7**: e33988.

Zhang H, Patana AS, Mackenzie PI, Ikushiro S, Goldman A, and Finel M (2012) Human UDP-glucuronosyltransferase expression in insect cells: ratio of active to inactive recombinant proteins and the effects of a C-terminal his-tag on glucuronidation kinetics. *Drug Metab Dispos* **40**: 1935-1944.

Zhang T, Haws P, and Wu Q (2004) Multiple variable first exons: a mechanism for cell- and tissue-specific gene regulation. *Genome Res* **14**: 79-89.

MOL #91462

Footnotes

This work was supported by the National Natural Science Foundation for the Youth of China [81302861]; the Program of Shanghai Subject Chief Scientist to QW; the Ministry of Science and Technology of China [2009CB918700]; the National Natural Science Foundation of China [31171015, 30970669]; the Science and Technology Commission of Shanghai Municipality [09PJ1405300].

For reprint requests: Qiang Wu, 800 Dongchuan Rd, Minhang, Shanghai 200240, China;

qw123@gmail.com

YW and HH contribute equally.

MOL #91462

Figure legends

Figure 1. Tissue-specific expression profiles of the zebrafish *Ugt* gene repertoire. The expression of the zebrafish *Ugt1* (A), *Ugt2* (B), and *Ugt5* (C) genes was measured by semiquantitative RT-PCR analyses using isoform-specific primers spanning at least one intron. The expression of the zebrafish β -actin gene (D) was used as a control. The position of each primer is indicated by an arrow and their sequences are listed in the Supplemental Table S1. The genomic organization of each cluster is shown above the respective panels. Yellow and green boxes represent variable exons and constant exons of *Ugt1* and *Ugt2*, respectively. Red and orange boxes represent exons of *Ugt5* and β -actin, respectively. Gray and blue boxes represent pseudogenes (*p*) or relics (*r*) and noncoding exons, respectively. Variants *u1* and *u2* refer to alternative splicing of different 5' noncoding exons upstream of *Ugt5b1* and *Ugt5b2*. The gene names are shown on the left. The tissue sources are indicated above each lane.

Figure 2. Expression (A) and Endo H treatment (B) of recombinant zebrafish UGT enzymes. Shown are Western blots of the recombinant zebrafish UGT superfamily (A). Multiple bands were rendered to a single band after the Endo H treatment (B). The name of each recombinant enzyme is indicated on the top of each lane. The molecular weights of the markers are indicated on the left of the panel.

Figure 3. High glucuronidation activities of zebrafish UGT1 and UGT2 enzymes. Shown are the HPLC chromatograms of strong glucuronidation activities of UGT1A1 toward 1-naphthol (A), BPA (B), MPA (C), and diclofenac (D); UGT1A3 toward MPA (E); UGT1A4 toward 4-MU (F); UGT1A7 toward 4-MU (G); UGT1B1 toward 4-NP (H) and E_2 (I); UGT1B7 toward bilirubin (J); UGT2B3 toward

MOL #91462

1-naphthol (K); and UGT2B6 toward 4-MU (L) with the mock control in the right half of each panel. The glucuronide peak for each substrate is indicated by an arrow. The chemical structure for each substrate is shown in the respective panel and the glucuronidation site is indicated in red color. Bilirubin-MG and bilirubin-DG refer to the mono- and di-glucuronides of bilirubin, respectively. The mV (millivolt) or mAU (milli Absorbance Unit) represents the measurement unit used by the fluorescence or UV detector, respectively.

Figure 4. UGT5 glucuronidation activities toward aglycone substrates with the donor UDPGA.

Shown are the HPLC chromatograms of glucuronidation activities of UGT5A toward t-OP (A); UGT5A5 toward 4-MU (B), 4-NP (C), 1-naphthol (D), t-OP (E), MPA (F), E₂ (G), testosterone (H), and diclofenac (I); UGT5B2 toward 4-MU (J), 4-NP (K), 1-naphthol (L), t-OP (M), and E₂ (N); UGT5C3 toward 4-MU (O) and t-OP (P); UGT5E1 toward 4-MU (Q), 4-NP (R), t-OP (S), E₂ (T), and testosterone (U). The black or grey lines represent glucuronidation assays of recombination proteins or mock controls, respectively. The chemical structures for t-OP, E₂, and testosterone and their glucuronidation sites are shown in the respective panel. The glucuronide peak for each substrate is indicated by an arrow. Some assays shared the same controls. The mV (milli Volt) or mAU (milli Absorbance Unit) represents the measurement unit used by the fluorescence or UV detector, respectively.

Figure 5. Kinetic analyses of recombinant zebrafish UGT enzymes toward the aglycone substrates

with high glucuronidation activities. Shown are the glucuronidation kinetic plots (main plots) created by using nonlinear fitting of experimental data of UGT1A1 toward 4-NP (A), 1-naphthol (B), BPA (C), MPA

MOL #91462

(D), and diclofenac (E); UGT1A7 toward 4-MU (F) and 4-NP (G); UGT1B1 toward 4-MU (H), 4-NP (I), 1-naphthol (J), MPA (K), and E₂ (L); UGT5A5 toward 1-naphthol (M) and t-OP (N); UGT5B2 toward t-OP (O); UGT5E1 toward E₂ (P) and testosterone (Q). Data in the panels A-H, J-L, and O-Q were fitted to the substrate inhibition equation (eq. 2); data in the panels I and M were fitted to the modified Hill equation (eq. 3); and data in the panel N was fitted to the Michaelis-Menten equation (eq. 1). The corresponding Eadie-Hofstee plot was shown in the inset of each panel.

Table 1
HPLC analytical conditions used for the UGT activity assays

Substrate	Eluent (A/B)	Flow rate (ml/min)	Temperature (°C)	Gradient	Detection (nm)	Quantitation
4-Methylumbelliferone	0.05% TFA/Methanol	0.6	40	20-100-100-20-20%B at 0-20-27-33-45 min	Fluorescence 315/365	Authentic standard
4-Nitrophenol	0.05% TFA/Methanol	0.6	40	20-100-100-20-20%B at 0-20-27-33-45 min	UV 320	Authentic standard
1-Naphthol	0.05% TFA/Methanol	0.6	40	20-100-100-20-20%B at 0-30-37-43-55 min	Fluorescence 290/330	Authentic standard
4-tert-Octylphenol	0.05% TFA/Acetonitrile	0.6	40	20-95-95-20-20%B at 0-30-37-43-55 min	Fluorescence 365/415	Parent compound absorbance
Estradiol	0.05% TFA/Acetonitrile	0.5	40	Isocratic 40%B	Fluorescence 210/300	Authentic standard
Testosterone	0.05% TFA/Acetonitrile	0.5	40	20-95-95-20-20%B at 0-30-37-43-55 min	UV 241	Parent compound absorbance
Bilirubin	50 mM Ammonium Acetate, pH3/methanol	0.7	25	60-75-75-95-95-60-60%B at 0-10-17-25-40-45-60 min	UV 453	Parent compound absorbance
Bisphenol A	0.05% TFA/Methanol	0.6	40	20-100-100-20-20%B at 0-30-37-43-55 min	UV 278	Parent compound absorbance
Mycophenolic acid	0.05% TFA/Methanol	0.6	40	20-100-100-20-20%B at 0-30-37-43-55 min	UV 250	Parent compound absorbance
Diclofenac	0.05% TFA/Acetonitrile	0.5	40	20-95-95-20-20%B at 0-30-37-43-55 min	UV283	parent compound absorbance

TFA, Trifluoroacetic Acid.

Table 2**Glucuronidation activities of recombinant zebrafish UGT proteins toward ten aglycone substrates**

	4-MU	4-NP	1-Naphthol	BPA	t-OP	MPA	E ₂ (3-G)	E ₂ (17-G)	Testosterone	Bilirubin	Diclofenac
UGT	Glucuronidation activity (<i>pmol/min/mg protein</i>)										
1A1	14.84±2.82	192.92±60.82	237.93±18.39	5.19±0.52	0.20±0.04	242.46±29.83	2.21±0.18	0	0	+	115.04±16.06
1A3	11.58±0.87	33.22±3.66	1.94±0.35	+	0.17±0.03	66.45±5.29	0	0	0	+	+
1A4	1.76±0.23	+	+	0	0	0	0	0	0	0	0
1A7	651.42±51.39	262.43±36.52	6.70±0.68	0	0	0	0	0	0	0	0
1B1	131.09±6.03	316.13±24.93	53.75±5.72	+	+	86.55±3.28	5.72±0.81	0	0	+	0
1B2	+	+	+	0	0	0	0	0	0	0	0
1B7	0	0	0	0	0	0	0	0	0	9.21±1.38	0
2B3	0.52±0.26	1.86±0.10	2.63±0.52	0	0	0	0	0	0	0	0
2B6	0.46±0.12	+	+	0	0	0	0	0	0	0	0
5A5	1.80±0.36	14.02±1.13	3.59±0.64	0	1.67±0.06	+	+	4.19±0.82	3.96±1.08	0	+
5B2	1.56±0.37	41.14±2.86	2.92±0.79	0	79.55±2.21	0	8.02±1.14	0	0	0	0
5C3	9.39±1.90	0	0	0	+	0	0	0	0	0	0
5E1	9.13±1.54	53.11±12.61	0	0	+	0	+	76.43±2.42	390.52±61.23	0	0

Data were normalized with relative enzyme levels and were expressed as mean ± S.D. derived from at least three determinations. Note that the substrate estradiol (E₂) is glucuronidated on two different positions of 3'-OH and 17'-OH. For enzymes of UGT1A2, 1A5, 1A6, 1B3, 1B4, 1B5, 2A1, 2A2, 2A3, 2A4, 2A5, 2A6, 2B1, 2B5, 5A1, 5A2, 5A3, 5B1, 5B3, 5B4, 5C1, 5C2, 5D1, 5F1, 5G1, and 5G2, there are no detectable glucuronidation activities toward any of the ten substrates examined. For UGT5A4, only trace activity was detected toward t-OP. 0: no detectable activity. +: trace activity.

Table 3
Kinetic analyses of six zebrafish UGT enzymes with nine aglycone substrates

UGT	Substrate	V_{\max}	$K_m(K_s)$	K_i	V_i	n	$CL_{\text{int}}(CL_{\text{max}})$	R^2
		<i>pmol/min/mg</i>	μM	μM	<i>pmol/min/mg</i>		$\mu\text{l/min/mg}$	
1A1	4-NP ^b	489.8±71.6	2428±542.9	6784±1852			0.20	0.9727
	1-Naphthol ^b	460.0±93.6	159.8±58.5	1845±1229			2.88	0.9779
	BPA ^b	26.4±2.3	106.7±15.8	510.9±102.9			0.25	0.9832
	MPA ^b	332.1±14.3	334.3±26.0	6573±1162			0.99	0.9985
	Diclofenac ^b	170.6±6.8	901.8±64.0	11051±1532			0.19	0.9992
1A7	4-MU ^b	855.2±74.1	142.4±22.2	2835±1056			6.01	0.9941
	4-NP ^b	471.2±46.0	764.5±116.8	2733±509.4			0.62	0.9958
1B1	4-MU ^b	250.0±20.3	17.7±2.46	94.8±15.3			14.1	0.9833
	4-NP ^c	659.6±43.4	281.9±28.4	1931±182.8	128.3±10.3	1.75±0.16	1.18	0.9959
	1-Naphthol ^b	88.3±5.6	47.6±4.5	243.0±40.4			1.86	0.9910
	MPA ^b	225.7±22.5	60.9±12.5	594.8±135.7			3.71	0.9631
	E ₂ ^{b,d}	8.82±0.77	93.6±14.4	1146±352.1			0.094	0.9957
5A5	1-Naphthol ^c	12.7±5.2	5316±2786	1655±612.7	0.78±0.11	1.11±0.08	0.0017	0.9987
	t-OP ^a	2.80±0.057	334.0±16.1				0.0084	0.9992
5B2	t-OP ^b	429.7±76.2	859.3±179.4	389.4±97.0			0.50	0.9986
5E1	E ₂ ^{b,d}	89.8±1.5	13.4±0.62	2579±647.7			6.70	0.9988
	Testosterone ^b	477.1±13.7	30.6±2.7	3422±608.9			15.6	0.9936

Kinetic parameters are shown as mean ± S.D. of parameter fit according to appropriate models. ^aMichaelis-Menten model, ^bSubstrate inhibition model, ^cSubstrate inhibition and Hill sigmoidal kinetics model, ^dThe kinetic constants of UGT1B1 and UGT5E1 toward estradiol (E₂) were tested on the positions 3'-OH and 17'-OH of estradiol, respectively.

Figure 1

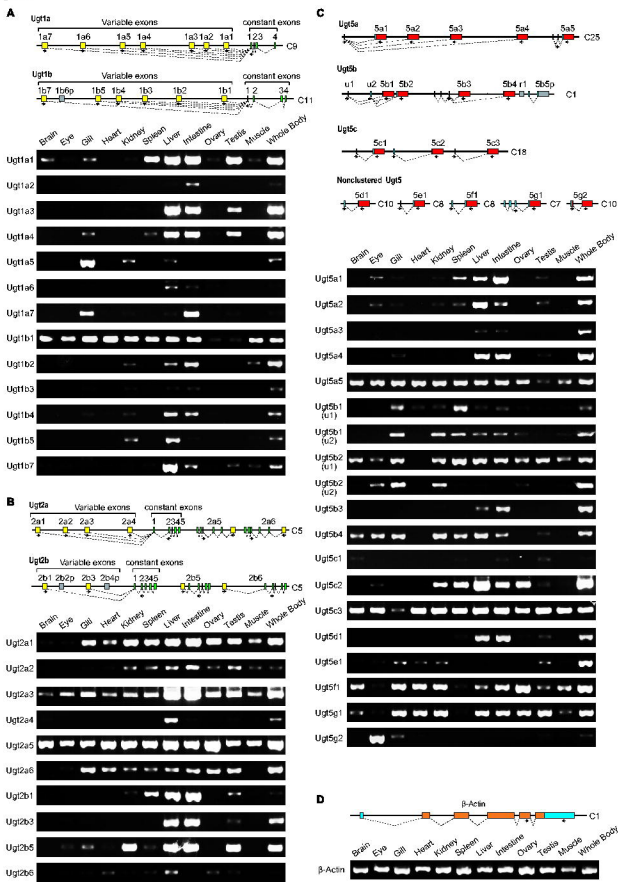


Figure 2

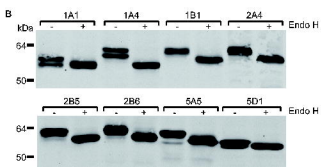
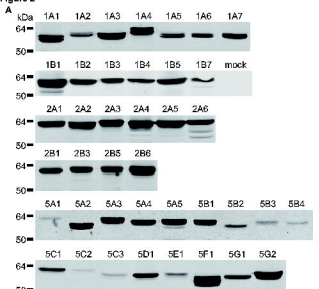


Figure 3

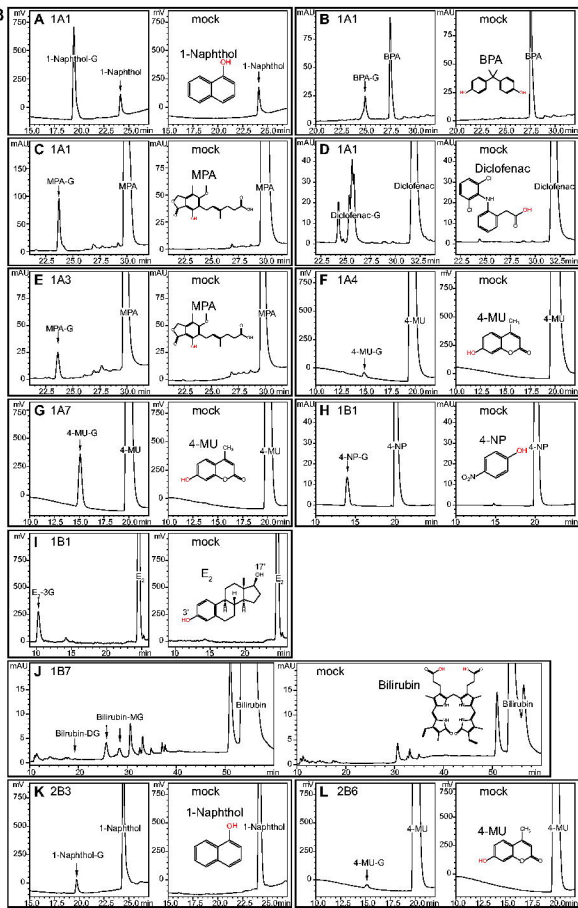


Figure 4

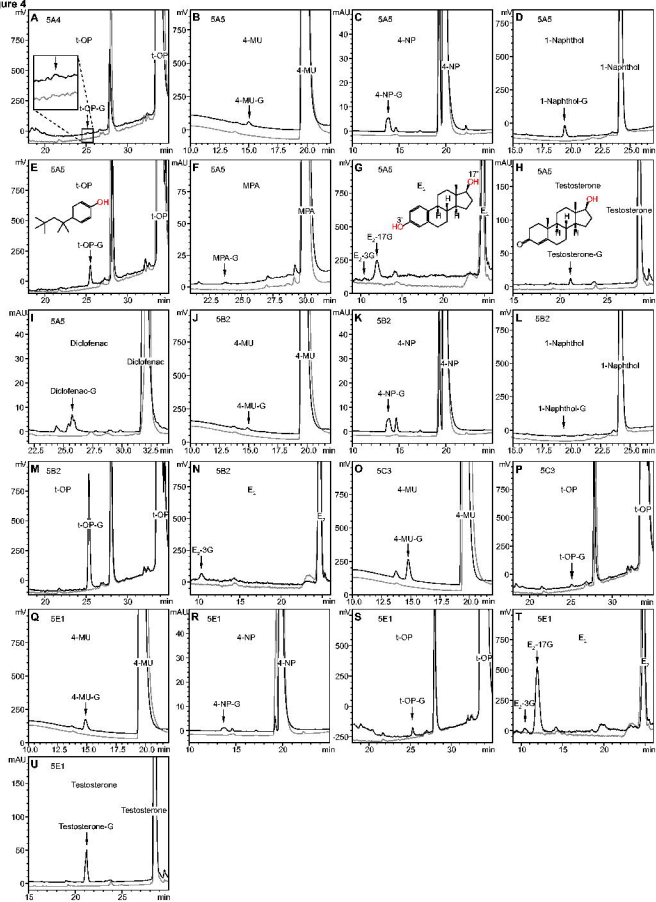


Figure 5

